Transactions, SMiRT-24
BEXCO, Busan, Korea - August 20-25, 2017
Division I

TRIAXIAL EXPANSION OF PLAIN, REINFORCED AND FIBER-REINFORCED ASR-AFFECTED CONCRETE

Daman K Panesar[1], and Bishnu P Gautam[2]

[1] Associate Professor, Department of Civil Engineering, University of Toronto, Canada
[2] Former Postdoctoral Fellow, Department of Civil Engineering, University of Toronto, Canada

ABSTRACT

Alkali-silica reaction (ASR) is a serious durability problem that may cause expansion, cracking and degradation in mechanical properties of concrete in nuclear structures. ASR expansion is volumetric and the axial expansion due to ASR can transfer from a restrained direction to the non-restrained directions. Furthermore, confinement, such as due to fibers, can be non-directional (volumetric). Reinforcement, either in the form of conventional reinforcing bars or in the form of fiber reinforcement, often reduces the expansion due to ASR. While concrete nuclear structures are reinforced concrete structures having reinforcing steel oriented in one or more directions, studies on ASR expansion, even for fiber-reinforced concrete (FRC), often rely on the measurement of the longitudinal expansion.

This study measures triaxial expansion of ASR-affected FRC to understand the effectiveness of steel fiber reinforcement on ASR expansion. Concrete specimens are made with reactive Spratt as the coarse aggregate. Expansion in FRC specimens is compared with those of plain concrete specimens and of specimens reinforced with a conventional reinforcing rod. It should be noted that the inclusion of steel fibers in concrete is usually defined in terms of fiber volume fraction and the inclusion of reinforcing steel is usually defined in terms of reinforcement ratio. While the effects of fibers and reinforcing steel on ASR expansion are explained based on these two parameters and are often disconnected, this study attempts to compare and contrast the roles of different forms of steel inclusion on ASR expansion based on the two parameters.

INTRODUCTION

Alkali-silica reaction (ASR) is a serious durability problem that may cause expansion, cracking and degradation in mechanical properties of concrete. Fiber-reinforced concrete (FRC) has been considered as a potentially suitable material for reducing the adverse effects of ASR on concrete including expansion, opening of cracks, and degradation of mechanical properties (de Carvalho et al. 2010; Giaccio et al. 2015; Ostertag et al. 2007; Yazici 2012).

Expansion measurement is perhaps the most popular tool to characterize ASR in concrete and it is mostly performed along the axial direction of unrestrained longitudinal specimens in laboratory studies. Similar practices of measuring longitudinal expansion have been adopted to assess the performance of ASR-affected FRC. Such studies have explained the ASR expansion of FRC to some extent, and some contradictory findings exist as to the effectiveness of fibers. While fibers are generally reported to reduce ASR expansion, longitudinal expansion due to ASR for prism (50 mm by 50 mm) specimens of concrete with steel fibers (0.5% and 1% by volume) was larger compared to the expansion of specimens without fibers (Haddad and Smadi 2004). This behaviour was attributed to the greater ductility of fiber-reinforced concrete, which allowed less cracking and more expansion (Haddad and Smadi 2004).

Ostertag et al. (2007) proposed that steel fibers produce chemo-mechanical confinement which reduces volumetric expansion of ASR gel and reduces the formation of ASR gel and the reactivity of aggregate. The chemical and mechanical confinement increased the viscosity of the ASR gel leading to a slower rate of reaction. Steel fibers were reported to reduce axial expansion of ASR-affected mortar (de

Carvalho et al. 2010). For concrete, Giaccio et al. (2015) reported that even though incorporation of fibers does not avoid ASR in concrete, some fibers may be useful to reduce in some extent the expansion rate and the magnitude. It appears that a clear understanding on the effect of fibers on ASR expansion is not possible because of the lack of studies of ASR expansion at the volumetric level.

ASR expansion is volumetric and the axial expansion due to ASR can transfer from a restrained direction to the non-restrained directions (Gautam et al. 2017). The study (Gautam et al. 2017) involved 254 mm size cube specimens that were made from reactive concrete and were subjected to no-stress, uniaxial, biaxial and triaxial compressive stresses during the evolution of ASR. The axial expansion in a particular direction (Z) was approximately 0.15% for the no-stress specimen, it was significantly increased to 0.3% for the biaxially stressed specimen because of stresses in the other two directions (X and Y), and it was significantly reduced to 0.03% in the triaxially stressed specimen because of the stress in all directions (X, Y and Z) (Gautam et al. 2017). Furthermore, the rate of free expansion of the concrete material as used in ASR-affected Gentilly-2 Nuclear Power Plant in Canada was 150 μm/m/year but the observed expansion at the biaxially confined containment walls was only 9 μm/m/year (Gocevski 2015). Since concrete in structures is often restrained in one or multiple directions, information on axial expansion is limited in understanding the ASR expansion in concrete structures. Furthermore, confinement, such as due to fibers, can be non-directional (volumetric) as they are conceivably oriented randomly in three-dimensional space. Reinforcement, either in the form of conventional reinforcing bars or in the form of fiber reinforcement, often reduces the expansion due to ASR. Therefore, effectiveness of fibers in reducing ASR expansion should be investigated by measuring volumetric expansion. This study measures expansion of ASR-affected plain, fiber-reinforced and conventionally reinforced concrete prism specimens in three mutually perpendicular directions. Expansion results are explained by considering that ASR expansion is a volumetric phenomenon.

REINFORCEMENT RATIO AND FIBER VOLUME FRACTION

Inclusion of steel reinforcement in concrete is expressed in terms of reinforcement ratio, the ratio of the cross-sectional area of reinforcement to the cross-sectional area of concrete in the given direction. Reinforcement ratio is a quantity based on area measurement in which a particular direction is either stated or implied. On the other hand, inclusion of steel fibers in concrete is expressed in terms of fiber volume fraction, the ratio of volume of fibers to the volume of concrete. Fiber volume fraction is a volumetric measurement; since fibers are generally assumed to be randomly distributed volumetrically, no particular direction is assigned when considering fiber volume fraction. Even though the effect of fibers or reinforcing steel on ASR expansion and cracking is often explained in terms of these two parameters, a possible connection is not understood between the cross-sectional areas of steel as expressed by the two parameters.

Theoretical and experimental studies exist which attempt to consider the cross-sectional area of fibers in a given direction by considering a parameter called fiber orientation factor (Soroushian and Lee 1990). For an infinite space, fiber distribution can be assumed random. Therefore, for a given cross-sectional area (**a**) of a fiber as shown in Figure 1, the component in one particular direction, say X, (a_x) can be given as:

$$a_x = a_{xy}\cos\beta = (\mathbf{a}\cos\alpha)\cos\beta = \mathbf{a}\cos\alpha\cos\beta \tag{1}$$

Considering that per unit volume of concrete contains N number of fibers and the fibers may have any orientation from 0 to 90°, the projected cross-sectional area of N fibers in X-direction is given as:

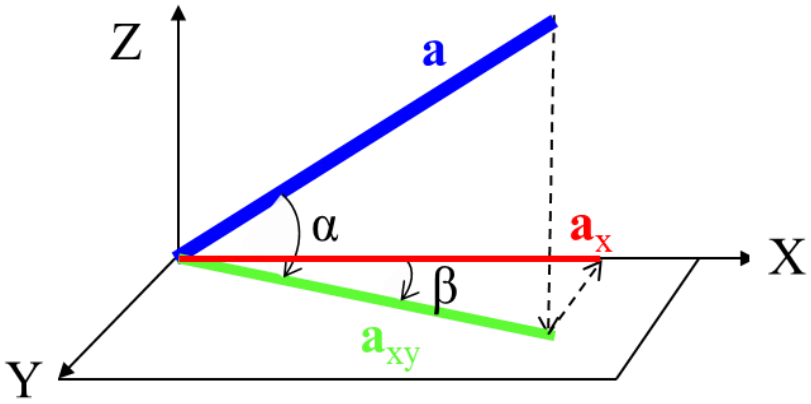

Figure 1.: Orientation of a fiber in concrete

$$A_x = N \times \text{average}\,(a_x) = N \frac{\int_0^{\frac{\pi}{2}} \int \mathbf{a} \cos\alpha \cos\beta}{\int_0^{\frac{\pi}{2}} \int \alpha\beta} = 0.405\, N\mathbf{a} = 0.405\,\mathbf{A} \qquad (2)$$

where **A** is the total cross-sectional area of *N* fibers. However, for a finite concrete volume, the boundary conditions restrict the freedom of fibers to orient randomly and the fibers tend to align along the boundaries (Soroushian and Lee 1990). Such an influence of the boundary conditions is dependent on the size and shape of the boundaries and the size of the fibers.

EXPERIMENTAL

Materials and Concrete Mix Design

Alkali-silica reactive concrete was used in this study. The mix design was based on ASTM C1293 (2015). The nominal maximum size of coarse aggregate was limited to the intermediate size (12.5 mm) range. As presented in Table 1, three concrete mixtures were produced by varying the fiber volume fraction as 0%, 0.65% and 1.3%. Accordingly, the three mixes were designated as M0.0, M0.65 and M1.3, respectively. Hooked end steel fibers with aspect ratio of 79 (30 mm length and 0.38 mm diameter) were used. The manufacturer specified tensile strength of the fibers was 3070 MPa.

Spratt aggregate was used as the reactive coarse aggregate. It is a siliceous limestone, crushed aggregate from a quarry in Ontario, Canada, and has been used as a reference aggregate to calibrate ASR test methods (Fournier et al. 2012). The non-reactive fine aggregate was natural sand from Milton, Ontario, Canada. Sand was tested for non-reactivity and passed the 14-day expansion limit of 0.1% as per ASTM C1260 (2014). The water-to-cement ratio was 0.44 for all mixes. High alkali general use (GU) cement was used with a total alkali content of 0.99 % Na_2O equivalent by mass of cement. The chemical composition of cement is shown in Table 2. The alkali level of the concrete mixes was increased to 5.25 kg/ m^3 Na_2O equivalent of concrete by adding NaOH pellets to water prior to concrete mixing.

Table 1: Mix designs of concrete (mass in kg for 1 m^3 concrete)

Material ↓ Mix →	M0.0	M0.65	M1.3
Cement	420	420	420
Coarse aggregate (Spratt) (12.5 – 9.5 mm) 50% (9.5 – 4.75 mm) 50%	1112	1112	1112
Water	185	185	185
Alkali pellet	1.4	1.4	1.4
Sand	688	688	688
Steel fiber	-	51	102
Note: Mixes M0.65 and M1.3 were obtained by adding fibers in the mix design similar for M0.0, without changing the mix design calculation to accommodate the fiber volume.			

Table 2: Chemical composition of GU cement

Constituents	LOI	SiO_2	Al_2O_3	Fe_2O_3	CaO	MgO	SO_3	Alkali (Na_2O_{eq})	Free Lime	Insoluble residue
Percentage	2.27	19.25	5.33	2.41	62.78	2.36	4.01	0.99	1.29	0.52

Casting and conditioning of the specimens

For M0.0 and M0.65 mixes, two series of concrete prism specimens were cast: one with a central reinforcing rod and the other without a reinforcing rod. Accordingly, five test series were studied from the three mixes, namely, M0.0-p, M0.0-r, M0.65-p, M0.65-r, and M1.3-p where "p" stands for plain and "r" stands for reinforced with a 6.4 mm dia. central threaded steel rod of cross-sectional area 20.5 mm^2. The reinforcement ratio of the reinforced concrete prism specimen in the longitudinal direction was 0.365%. The specified tensile strength of the rod was 655 MPa.

For a concrete prism of size 285 mm × 75 mm × 75 mm and the length of fibers as 30 mm, the fiber orientation factor along the longitudinal direction of the prism was obtained as 0.5625 and along the transverse direction was 0.5 (Soroushian and Lee 1990). Therefore, a fiber volume fraction of 0.65% would be equivalent to a reinforcement ratio of 0.365%. By ignoring the type of steel inclusion, both a reinforcing rod with a cross-sectional area of 20.5 mm2 and a fiber volume fraction of 0.65% for 30 mm long and 0.38 mm diameter fibers would possess an identical equivalent reinforcement ratio of 0.365% in the longitudinal direction. Thus, M0.65-p and M0.0-r specimens had an equivalent reinforcement of 0.365% in the longitudinal direction, and M0.65-r and M1.3-p specimens had an equivalent reinforcement ratio of 0.73% in the longitudinal direction.

Concrete prisms were cast by following the procedures outlined in ASTM C1293 (2015). Five prisms were cast for each of the five test series. In the prisms of "p" series, steel studs were embedded in the ends of the prisms with a gauge length of 250 mm for measuring longitudinal expansion of the concrete core. In the prisms of "r" series, the ends of the central reinforcing rod were finished as the expansion measuring studs and thus the entire length of the concrete prism (285 mm) would be the gauge length for expansion measurement.

Specimens were demolded after one day of casting. After demolding, the prism specimens were partially drilled on four surfaces to insert expansion measurement studs along the two transverse directions. As shown in Figure 2, approximately 6 mm length of the 13 mm long expansion studs were embedded in

the drilled holes and the studs were glued in position by using epoxy adhesive. Moreover, Demec gauge points were glued on two surfaces of prisms with a gauge length of 200 mm to measure the surface expansion of concrete in the longitudinal direction. Concrete surface was scrubbed with a steel scrubber and was cleaned with acetone before gluing the Demec points with epoxy glue. The initial measurement of expansion was taken in three days of casting and the prisms were stored in hermetically sealed plastic pails and were conditioned under a constant temperature of 50±2 °C. Prior to performing the tests on the specimens, the pails were acclimatized at room temperature for 16 to 20 hours.

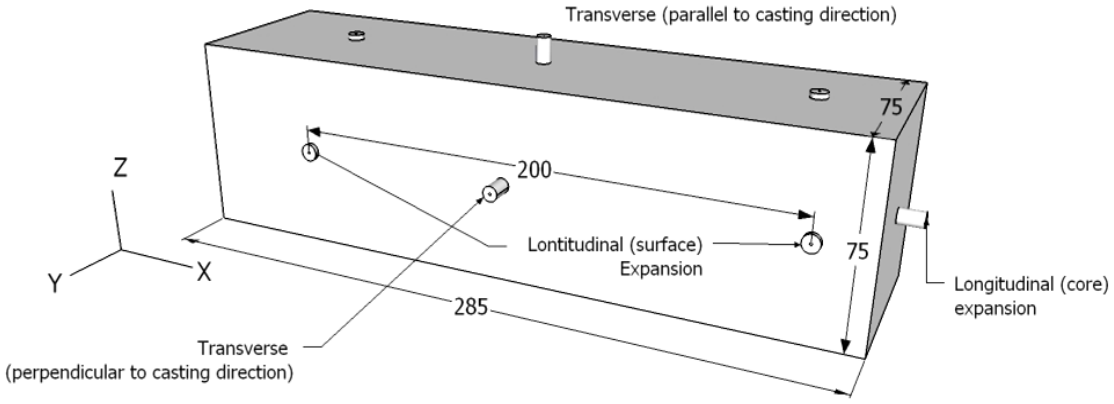

Figure 2. Arrangements of expansion measurement in a concrete prism. Note, the casting direction was along the Z-direction. (dimensions are in mm).

Test Details

Longitudinal expansion (core): The longitudinal expansion of concrete core was measured using a comparator against the steel studs embedded in the ends of the prisms with a gauge length of 250 mm. The gauge length for the reinforced concrete specimens (M0.0-r and M0.65-r) was 285 mm as the expansion measurement studs in these cases were the ends of the reinforcing rod that was continuously bonded with concrete for the full length of the prism specimens. The comparator had a resolution of 1 μm, and was calibrated with a reference invar bar. The initial reading for the longitudinal expansion of the prisms was taken at the age of three days. The prisms were subsequently measured for the longitudinal expansion at ages of 7, 28, 56, and 91 days.

Longitudinal expansion (surface): The concrete prisms were tested for longitudinal surface expansion. As shown in Figure 2, the expansion was measured using a Demec gauge against a pair of glued Demec points on the surface of the prisms. A digital gauge was used with a resolution of 1 μm. Two concrete surfaces were measured and the surface expansion was reported as the average expansion of the two surfaces. The initial reading for the longitudinal surface expansion of the prisms was taken at the age of three days. The prisms were subsequently measured for the longitudinal surface expansion at ages of 7, 28, 56, and 91 days.

Transverse expansion: As shown in Figure 2, transverse expansion of concrete prisms was measured in two directions, namely, parallel to the casting direction (against one formed and one finished surface) and perpendicular to the casting direction (against two formed surfaces). Transverse expansion was measured by using a digital microscope with a resolution of 1 μm. The gauge length was obtained by subtracting two lengths of studs from the total measurement. The initial reading for the transverse expansion of the prisms was taken at the age of three days. The prisms were subsequently measured for transverse expansion at ages of 7, 28, 56, and 91 days.

RESULTS AND DISCUSSION

Longitudinal (Core) Expansion

Longitudinal (core) expansions of the concrete prisms for the five series are shown in Figure 3. As shown in the figure, the core expansion was reduced with an increase in fiber content. For the three series with no reinforcing rod, the order of expansion was M0.0-p > M0.65-p > M1.3-p. Compared to M0.0-p specimens with no fibers, the expansion at 91 days was reduced by about 20% in M0.65-p specimens (with 0.65% fiber volume fraction) and 45% in M1.3-p specimens (with 1.3% fiber volume fraction). Reduction in longitudinal expansion with an increase in fiber content was observed also for the prisms with a reinforcing rod as M-0.65-r series showed lower expansion compared to M0.0-r series.

The core expansion of both reinforced prisms was significantly smaller compared to the prisms without a reinforcing rod. At 91 days, expansion of M0.0-r was lower than that of M0.0-p by approximately 48% and expansion of M0.65-r was lower than that of M0.65-p by approximately 45%. It should be noted that as the expansion was measured directly on the axis of the reinforcing rod; the restraint provided by the rod caused the measured expansion to underestimate the average longitudinal expansion of the prism. In order to understand this influence, the longitudinal expansion was also measured on the surface of prisms, which is explained in the following section.

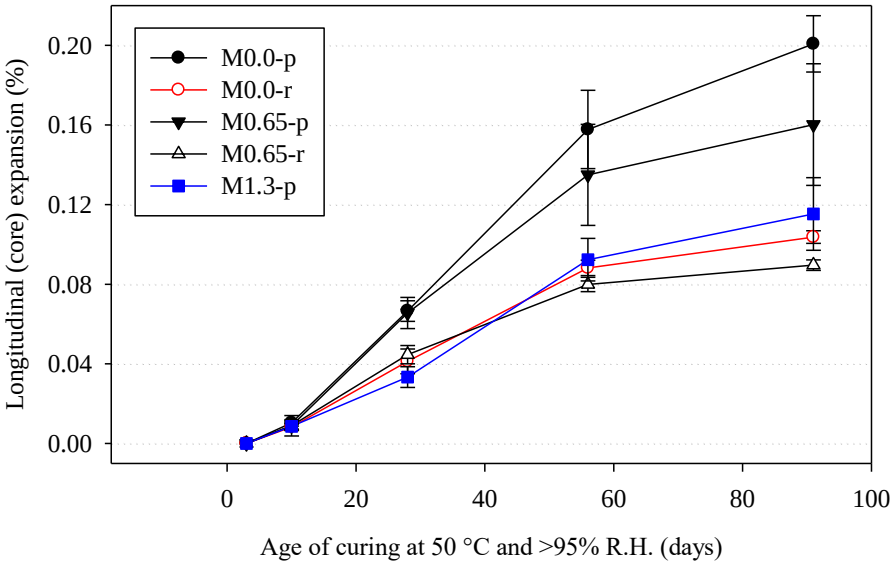

Figure 3. Longitudinal (core) expansion of concrete prism specimens

When comparing M0.0-r vs. M0.65-p (equivalent reinforcement ratio of 0.365%) and M0.65-r vs. M1.3-p (equivalent reinforcement ratio of 0.73%), reinforcing rod was more effective to restrain the ASR expansion when compared to fibers. This observation can be explained by the deformable and rigid body motions of the steel inclusions. While fibers elongate due to ASR, fibers do span a relatively smaller region of concrete and also undergo some rigid body movement along with the expanding concrete. On the other hand, the reinforcing rod spans the whole length of concrete and could elongate due to ASR but not undergo the rigid body movement.

Longitudinal (Surface) Expansion

Longitudinal (surface) expansions of the concrete prisms for the five series are shown in Figure 4. As shown in the figure, the greatest surface expansion occurred in M0.0-p specimens with no restraints, and the least surface expansion occurred in M1.3-p specimens with 1.3% fiber content. The results in Figure 3 and Figure 4 are compared in Table 3 in terms of the ratio of core to surface expansion. (The extremely large value for M0.0-p specimen at 7 days should be discarded considering extremely small values of the measurement). A value greater than 1 indicates greater core expansion compared to the surface expansion. The surface expansion for M0.0-p, M0.65-p and M1.3-p specimens was always lower compared to the core expansion. This observation suggests that the surface of ASR-affected concrete is subjected to drying due to exposure and expands relatively less when compared to the core. However, the surface expansion of M0.0-r and M0.65-r specimens was greater than their body expansion. Since the body expansion was measured directly on the axis of the reinforcing rod, the restraining effect due to the reinforcement influenced the body expansion in these latter specimens. The measured body expansion can be taken as the compatible expansion of the reinforcing rod and the surrounding concrete. The comparison of core and surface expansion suggested that even for a relatively smaller cross-section of concrete prisms, longitudinal expansion in not uniform across the cross-section. Therefore, monitoring of expansion in concrete structures may require particular attention to the non-uniformities in expansion associated with reinforcing rods.

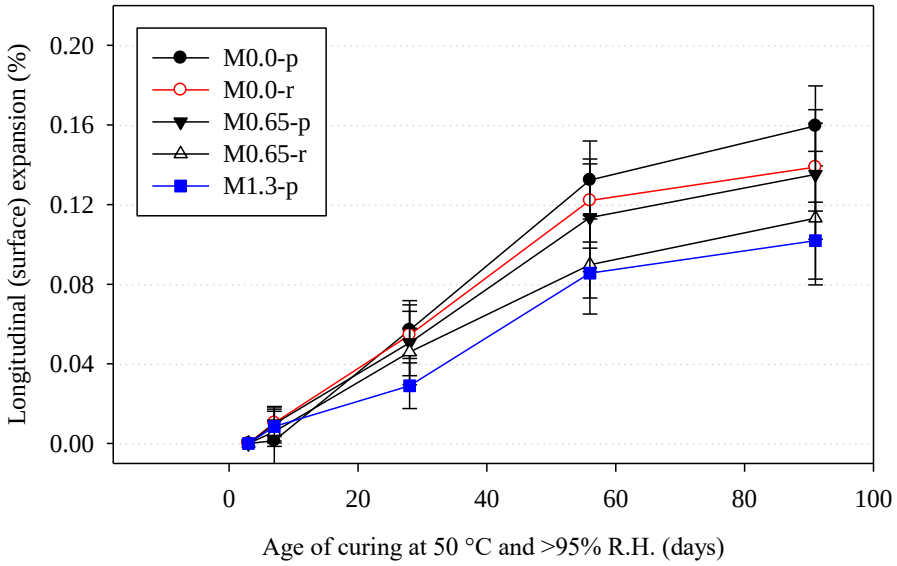

Figure 4. Longitudinal (surface) expansion of concrete prism specimens

Table 3: Comparison of core and surface expansion of concrete prisms

Age (days)	**Ratio of core to surface expansion**				
	M0.0-p	M0.0-r	M0.65-p	M0.65-r	M1.3-p
7	7.62	0.80	0.91	1.53	1.00
28	1.17	0.76	1.30	0.97	1.15
56	1.19	0.72	1.17	0.89	1.08
91	1.26	0.75	1.17	0.79	1.11

Transverse Expansion

Figure 5 shows the transverse expansion of prism specimens. The expansion results are the average of transverse expansions in the directions parallel and perpendicular to the casting direction. The transverse expansion is the lowest for M0.0-p specimens for which the longitiduanal expansion was completely unrestrained. The specimens with reinforcing rod or fibers exhibited greater transverse expansion when compared to the unrestrained specimen. Transverse expansion for M0.65-p, M0.65-r and M1.3-p specimens (which had some restraining due to fibers in the transverse direction) were close to each other and was lower than the transverse expansion of M0.0-p specimen which had no restraint in the transverse direction. The larger transverse expansion in the restrained specimens compared to the unrestrained specimen exihibited the phenomenon of transfer of ASR expansion from the restrained to unrestrained direction (Gautam et al. 2017).

Compared to the longitudinal expansion, the specimens underwent significantly larger transverse expansions. This could be associated mainly to the aspect ratio of the specimen as was previously reported (Gautam and Panesar 2014). Even for M0.65-p and M1.3-p specimens, which had fiber restraints in the transverse direction, the degree of restraint due to fibers was greater along the longitudinal direction than in the transverse direction (fiber orientation factor of 0.5625 vs. 0.50 in the longitudinal and transverse directions). For a given fiber volume fraction of concrete, the relatively larger orientation factor in the longitudinal direction caused greater restraint in ASR expansion in the longitudinal direction compared to the transverse direction. A relatively large scatter in the measurement of transverse expansion must have been resulted mostly because the measurement was taken for a relatively small gauge length of approximately 63 mm.

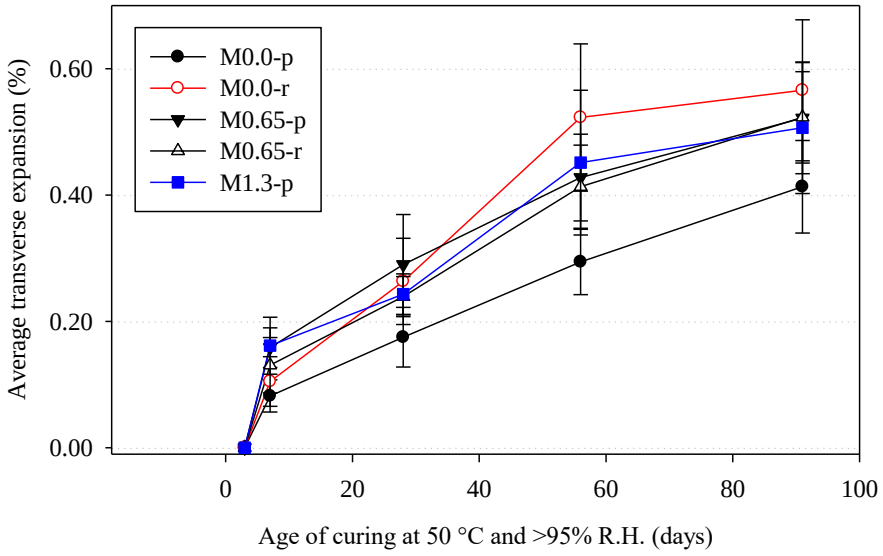

Figure 5. Transverse expansion of concrete prism specimens

Volumetric Expansion

Figure 6 shows the volumetric expansion of prism specimens. The volumetric expansion was obtained by adding the longitudinal (core) expansion, the transverse expansion parallel to the casting direction and the transverse expansion perpendicular to the casting direction. The non-uniform cross-sectional expansion has been ignored but such non-uniformities might have some influence on the results.

As shown in Figure 6, the volumetric expansion was the lowest for the unrestrained M0.0-p specimens and greatest for the M0.0-r specimens with no restraints in the transverse directions. An increased volumetric expansion of uniaxially stressed specimen when compared to a no-stress specimen was also observed previously (Gautam 2016; Gautam et al. 2017). Volumetric expansion of specimens with fibers and reinforcing rod in this study (M0.65-p, M0.65-r and M1.3-p specimens) was larger when compared to the unrestrained M0.0-p specimen. While longitudinal expansion was reduced due to fibers or reinforcement in M0.65-p, M0.65-r and M1.3-p specimens as shown in Figure 3, the reinforcing rod or the fibers were unable to restrain the ASR expansion volumetrically. This observation suggests that comparison of longitudinal expansion alone is inadequate in assessing the effectiveness of fibers in reducing ASR expansion and a volumetric perspective is essential.

Gautam et al. (2017) suggested that ASR expansion tries to conserve volumetrically, and a hydrostatic stress lower than 1.5 MPa is unlikely to reduce volumetric expansion. Figure 3 indicates that the maximum elongation (expansion) of the reinforcing rod in M0.0-r specimen was 0.1%. Corresponding to the modulus of elasticity of steel as 200 GPa, this strain is equivalent to a tensile stress of 207 MPa in the reinforcing rod. For a reinforcement ratio of 0.365%, this tensile stress caused an average compressive stress of 0.76 MPa in concrete. For M0.65-r specimen, the maximum elongation was 0.09%, which corresponded to a tensile stress of 179 MPa. If the type of steel inclusion is ignored and an equivalent reinforcement ratio is considered, the equivalent reinforcement ratio in the longitudinal direction was 0.73% for M0.65-r specimen. For this equivalent reinforcement ratio, the tensile stress in steel produced an average compressive stress of 1.3 MPa in concrete for equilibrium. This stress level is lower than 1.5 MPa and hence, reduction in volumetric expansion was unlikely. However, unlike the case of reinforcing rod, the elongation of steel fibers is conceivably lower than the expansion of concrete and the steel fibers of similar equivalent reinforcement ratio may not produce as much stress as the reinforcing rod would do. Therefore for M1.3-p specimen, even though the equivalent reinforcement ratio of 0.73% and the maximum longitudinal expansion of 0.12% would suggest an average compressive stress of 1.7 MPa in the longitudinal direction, the average compressive stress in concrete might not have exceeded 1.5 MPa. A numerical simulation of the experimental results in this study may be useful to explain the likely stress state in the concrete specimens.

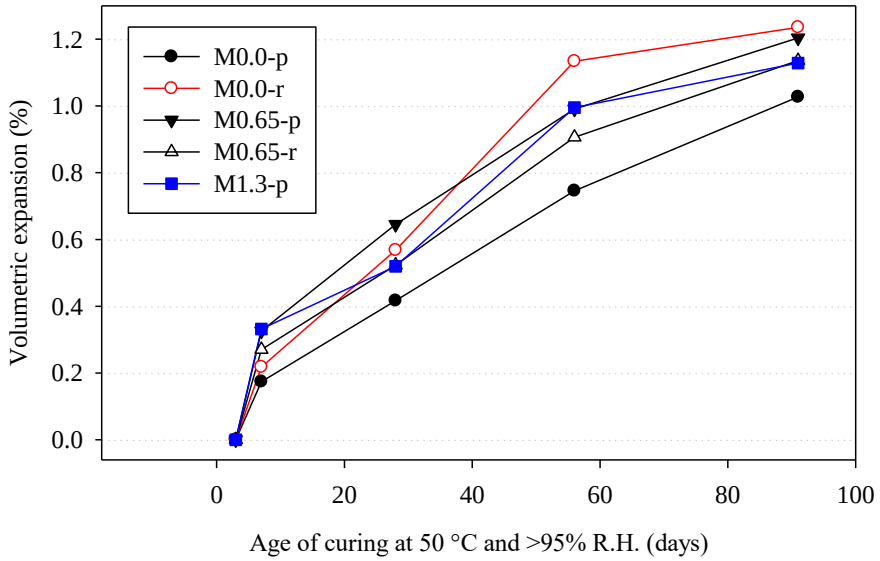

Figure 6. Volumetric expansion of concrete prism specimens

CONCLUSION

This study measured triaxial expansion of three types of ASR-affected concrete, namely, plain concrete, fiber-reinforced concrete and reinforced concrete with and without fibers. Concrete prism specimens were made with reactive Spratt as the coarse aggregate. Expansion in fiber-reinforced specimens was compared with those of plain concrete specimens and of specimens reinforced with a conventional reinforcing rod. While the longitudinal expansion was reduced due to steel fibers, the reinforcing rod and the steel fibers were inadequate to reduce volumetric expansion. Rather restrained specimens exhibited larger volumetric expansion when compared to unrestrained specimen.

While the effect of fibers in changing longitudinal expansion has been widely study, this study investigated the effect of fibers on the volumetric expansion of ASR and indicated that the effectiveness of fibers in reducing ASR expansion should be considered at volumetric level. The results from this study could be simulated through a numerical study and useful insights will be obtained in assessing the expansion of ASR-affected concrete structures that have stresses and restraints in one or more directions.

REFERENCES

ASTM C1260. (2014). *Standard test method for potential alkali reactivity of aggregates (mortar-bar method)*. ASTM International, West Conshohocken, PA.

ASTM C1293. (2015). *Standard test method for determination of length change of concrete due to alkali-silica reaction*. ASTM International, West Conshohocken, PA.

de Carvalho, M. R. P., Fairbairn, E. de M. R., Filho, R. D. T., Cordeiro, G. C., and Hasparyk, N. P. (2010). "Influence of steel fibers on the development of alkali-aggregate reaction." *Cement and Concrete Research*, 40(4), 598–604.

Fournier, B., Rogers, C. A., and MacDonald, C. (2012). "Multilaboratory study of the concrete prism and accelerated mortar bar expansion tests with Spratt aggregate." *14th International Conference on Alkali Aggregate Reaction*, Texas, USA, 10.

Gautam, B. P. (2016). "Multiaxially loaded concrete undergoing alkali-silica reaction (ASR) (PhD thesis)." University of Toronto.

Gautam, B. P., and Panesar, D. K. (2014). "Anisotropic expansion of ASR affected concrete prism specimens." *Proceedings of the XIII International Conference on Durability of Building Materials and Components*, M. Quattrone and V. M. John, eds., RILEM, Sao Paulo, 837–844.

Gautam, B. P., Panesar, D. K., Sheikh, S. A., and Vecchio, F. J. (2017). "Multiaxial Expansion-Stress Relationship for Alkali Silica Reaction-Affected Concrete." *ACI Materials Journal*, 114(1), 171–184.

Giaccio, G., Bossio, M. E., Torrijos, M. C., and Zerbino, R. (2015). "Contribution of fiber reinforcement in concrete affected by alkali-silica reaction." *Cement and Concrete Research*, Elsevier Ltd, 67, 310–317.

Gocevski, V. (2015). *Pathologies/degradation mechanisms experienced by Hydro-Quebec during the evaluation of Gentilly-2 NPP*. Hydro-Quebec, Montreal, Canada.

Haddad, R. H., and Smadi, M. M. (2004). "Role of fibers in controlling unrestrained expansion and arresting cracking in Portland cement concrete undergoing alkali-silica reaction." *Cement and Concrete Research*, 34(1), 103–108.

Ostertag, C. P., Yi, C., and Monteiro, P. J. M. (2007). "Effect of Confinement on Properties and Characteristics of Alkali-Silica Reaction Gel." *ACI Materials Journal*, 104(3), 276–282.

Soroushian, P., and Lee, C. D. (1990). "Distribution and orientation of fibers in steel fiber reinforced concrete." *ACI Materials Journal*, 87(5), 433–439.

Yazici, H. (2012). "The effect of steel micro-fibers on ASR expansion and mechanical properties of mortars." *Construction and Building Materials*, 30, 607–615.